D. M. Gokhfeld, D. A. Balaev, M. I. Petrov, S. I. Popkov, K. A. Shaykhutdinov, and V. V. Val'kov

View Online   **Export Citation**

ARTICLES YOU MAY BE INTERESTED IN

Magnetization asymmetry of type-II superconductors in high magnetic fields

D. M. Gokhfeld,[a)] D. A. Balaev, M. I. Petrov, S. I. Popkov, K. A. Shaykhutdinov, and V. V. Val'kov

L. V. Kirensky Institute of Physics SB RAS, Akademgorodok 50/38, Krasnoyarsk 660036, Russia

Inhomogeneous distribution of the pinning force in superconductor results in a magnetization asymmetry. A model considering the field distribution in superconductor was developed and symmetric and asymmetric magnetization loops of porous and textured $Bi_{1.8}Pb_{0.3}Sr_{1.9}Ca_2Cu_3O_x$ were fitted. It is found that the thermal equilibrium magnetization realizes in crystals smaller than some size depending on temperature and magnetic field. © *2011 American Institute of Physics.* [doi:10.1063/1.3544038]

I. INTRODUCTION

Critical characteristics of superconductors may be derived from the dependence of magnetization M on magnetic field H. However, many factors affect the shape of the hysteretic $M(H)$ curve. The same sample can have a various magnetization loop shape then it has been measured at different temperatures or up to different values of the maximal magnetic field. Also the geometric shape of the sample, its structure and homogeneity influence on the $M(H)$ dependence.[1,2]

At temperatures higher than ~ 10 K the high-field $M(H)$ dependencies of high-T_c superconductors have a pronounced asymmetry with respect to the $M=0$ axis, so the main parts of hysteretic loops locate in the second and the fourth quadrants. This asymmetry grows with increasing temperature. The critical state model was subjected to modifications to treat the asymmetric $M(H)$ dependencies.[3–5] Chen *et al.*[6] following approach[7] considered the total magnetization as the result of both the surface and the volume supercurrents, so the equilibrium magnetization and the surface barrier were included. As suggested in Ref. 6, the surface layer of a bulk sample, with a thickness of the order of the London penetration depth, is always in equilibrium. In the remnant volume of the sample the critical state model can be used with modified boundary conditions.[6] The extended critical model was studied and developed in the past years.[8–11] However, some aspects of the extended critical state model, e.g., presence of the surface equilibrium layer, were questionable from experimental point of view. So we were interested to treat the asymmetric magnetization loops by using some different approach. Earlier, variant of the critical state approach[12] was successfully applied for symmetric hysteretic loops of Tl1223 and Bi2223 measured at low temperature.[12,13] In this article, we have reexamined the model[12] and have modified it to fit the asymmetric magnetization loops. The resulted model explains origin of the $M(H)$ asymmetry and gives results consistent with that of Ref. 6. The asymmetric $M(H)$ dependencies of the porous high-T_c superconductor and textured one with the same chemical composition were fitted by the model. Our approach on the $M(H)$ dependencies is described in Sec. II. In Sec. III the magnetization loops of porous and textured $Bi_{1.8}Pb_{0.3}Sr_{1.9}Ca_2Cu_3O_x$ samples are presented. Discussion and conclusion are given in Sec. IV.

II. MODEL

All realizing $M(H)$ dependencies of superconductors are distributed between two extreme cases: a symmetric magnetization loop and a fully reversible $M(H)$ curve. Symmetry of $M(H)$ curve means that $M^-(H)=-M^+(H)$ at high H except region near maximal applied field H_m, where $M^-(H) \leq 0$ is the branch of magnetization curve measured during the field increasing from 0 to H_m, $M^+(H)$ is the branch of magnetization curve measured during the field decreasing H_m to 0. Symmetric $M(H)$ dependencies are observed at low temperatures when a strong pinning of the vortices realizes. If there is no pinning in the sample then the $M(H)$ dependence is fully reversible, $M^-(H)=M^+(H)$ for any H. The reversible $M(H)$ dependencies are observed for clean superconductors. High-T_c superconductors demonstrate crossover from the symmetric magnetization curves at low T to the reversible $M(H)$ dependencies at high T while pinning force decreases.

The critical state model describes successfully symmetric $M(H)$ dependencies in high magnetic fields. In version[12] it includes the following points:

(i) Magnetization of the material, which consists of a large number of cylindrical granules, described by the statistical ensemble $\varphi(R)$, is determined by

$$4\pi M(H) = -H + (1-P)\mu_n H + 2/R_0^2 \int_0^\infty \varphi(R) \int_0^R rB(r)drdR, \quad (1)$$

where P is the fraction of the material concentrated in the superconducting granules, μ_n is the magnetic permeability of the intergranular material, $\varphi(R)$ is the distribution density of the superconducting granules with respect to the radius R, $B(r)$ is the magnetic in-

duction in the sample. A homogeneous sample is described by (1) with $P=0$ and $R_0=R$.

(ii) The distribution of the magnetic induction $B(r)$ in the granule is deduced from the critical state equation $dB(r)/dr = \pm (4\pi/c)j_c(B)$, where j_c is the critical current density. Separate sets of Eqs. (2a) and (2c) are resulted for three main parts of the $M(H)$ hysteresis.

(1) During the initial field increasing from 0 to H_m, the $B(r)$ dependence is determined by equation

$$\Phi(B) - \Phi(\mu_n H) = -(4\pi/c)j_{c0}(R-r). \tag{2a}$$

(2) For decreasing H from H_m to 0 (i.e., $M^+(H)$ branch), the $B(r)$ dependence consists of two curves which are described by equations

$$\Phi(B) - \Phi(\mu_n H) = (4\pi/c)j_{c0}(R-r),$$

$$\Phi(B) - \Phi(\mu_n H_m) = -(4\pi/c)j_{c0}(R-r). \tag{2b}$$

(3) Then, for changing H from 0 to $-H_m$ [i.e., $M^-(H)$ branch], the $B(r)$ dependence consists of three parts

$$\Phi(-B) - \Phi(-\mu_n H) = -(4\pi/c)j_{c0}(R-r),$$

$$\Phi(B) + \Phi(-\mu_n H) = (4\pi/c)j_{c0}(R-r),$$

$$\Phi(B) - \Phi(\mu_n H_m) = -(4\pi/c)j_{c0}(R-r). \tag{2c}$$

Here j_{c0} is the critical current density at $H=0$, $\Phi(B)$ is a nondecreasing function, such that $d\Phi(B)/dB = [j_c(B)/j_{c0}]^{-1}$.[12]

The critical state model implies the strong pinning of vortices in a sample. In reality some distribution of the pinning force $F_p(r)$ is realized in granules since the magnetic field varies within the granule. Therefore, a region near granule surface can appear at high T and high H, where F_p is such small that vortices are not pinned. So the thermal equilibrium magnetization is produced by the surface supercurrent circulating in this region while vortices are pinned in the granule core only. This idea is coincide with assumption.[6,7]

Equations (2a)–(2c) should be modified to account the equilibrium magnetization. We introduce new characteristic size l_s determining the depth of surface layer where the vortices are not pinned. Then new equation for the $B(r)$ distribution in the equilibrium surface region is added. Also boundary conditions are changed for the first equation in each set (2a)–(2c) due to the surface supercurrent

$$\Phi(B) - \Phi(\mu_n H) = -(4\pi/c)j_{s0}(R-r),$$

$$\Phi(B) - \Phi(B_s) = -(4\pi/c)j_{c0}(R-r-l_s), \tag{3a}$$

$$\Phi(B) - \Phi(\mu_n H) = -(4\pi/c)j_{s0}(R-r),$$

$$\Phi(B) - \Phi(B_s) = (4\pi/c)j_{c0}(R-r-l_s),$$

$$\Phi(B) - \Phi(\mu_n H_m) = -(4\pi/c)j_{c0}(R-r), \tag{3b}$$

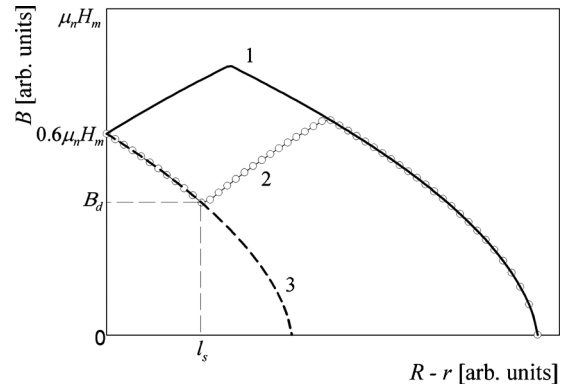$$\Phi(-B) - \Phi(-\mu_n H) = -(4\pi/c)j_{s0}(R-r),$$

FIG. 1. Dependence of induction B on depth $R-r$ from the granule surface after field decreased from H_m to $0.6H_m$ for $l_s=0$ (curve 1, solid line), $0 \leq l_s \leq R$ (curve 2, circles), and $l_s=R$ (curve 3, dotted line).

$$\Phi(-B) - \Phi(|B_s|) = -(4\pi/c)j_{c0}(R-r-l_s),$$

$$\Phi(B) + \Phi(-\mu_n H) = (4\pi/c)j_{c0}(R-r),$$

$$\Phi(B) - \Phi(\mu_n H_m) = -(4\pi/c)j_{c0}(R-r), \tag{3c}$$

here j_{s0} is the surface critical current density at $H=0$, B_s is the induction value at $r=R-l_s$. The separate notation for j_s is introduced here[9] that conforms to approach.[6] However, we suppose that in most cases $j_s=j_c$.[8]

Figure 1 displays the computed $B(r)$ dependencies after the field decreasing from H_m to $0.6H_m$. Curve 1 on Fig. 1 (solid line) is the $B(r)$ dependence for $l_s=0$, curve 2 (circles) is the $B(r)$ dependence for $0 \leq l_s \leq R$, curve 3 on Fig. 1 (dotted line) is the $B(r)$ dependence for $l_s \geq R$. The $B(r)$ distributions in Fig. 1 were calculated with the $j_c(B)$ dependence characterized by qualitatively different behaviors in scales of low and high fields[12]

$$j_c(B) = \frac{j_{c0}}{\dfrac{1+QB/B_1}{1+B/B_1} + \left(\dfrac{B}{B_0}\right)^g}, \tag{4}$$

where j_{c0} is the critical current density at $B=0$, B_1 and B_0 are the parameters with the induction measure which determine the characteristic scales. Dimensionless parameters $Q>0$ and $g>0$ determine the j_c decrease rate. Such $j_c(B)$ dependence is convenient because it is easy integrated.

Some $M(H)$ dependencies computed by the obtained model are presented in Figs. 2 and 3. This model is strongly adequate for the $M(H)$ dependencies in high fields. The additional pinning should appear near surface at low fields due to the surface (Bean–Livingston) barrier. The surface barrier should be account for detailed calculation of low-field magnetization as it was realized in Ref. 6. In contrast to the model,[6] the presented variant of the extended critical state model accounts l_s, the position of the boundary between the equilibrium layer and the central core with strong pinning.

The size of region, where pinning is missing, l_s, depends on H and T. If the condition $l_s/R \geq 1$ takes place for granules, the width of the magnetization loop $|M^-(H) - M^+(H)|$ is equal to 0. The crossover from the symmetric magnetization to the reversible $M(H)$ dependence can be observed while l_s
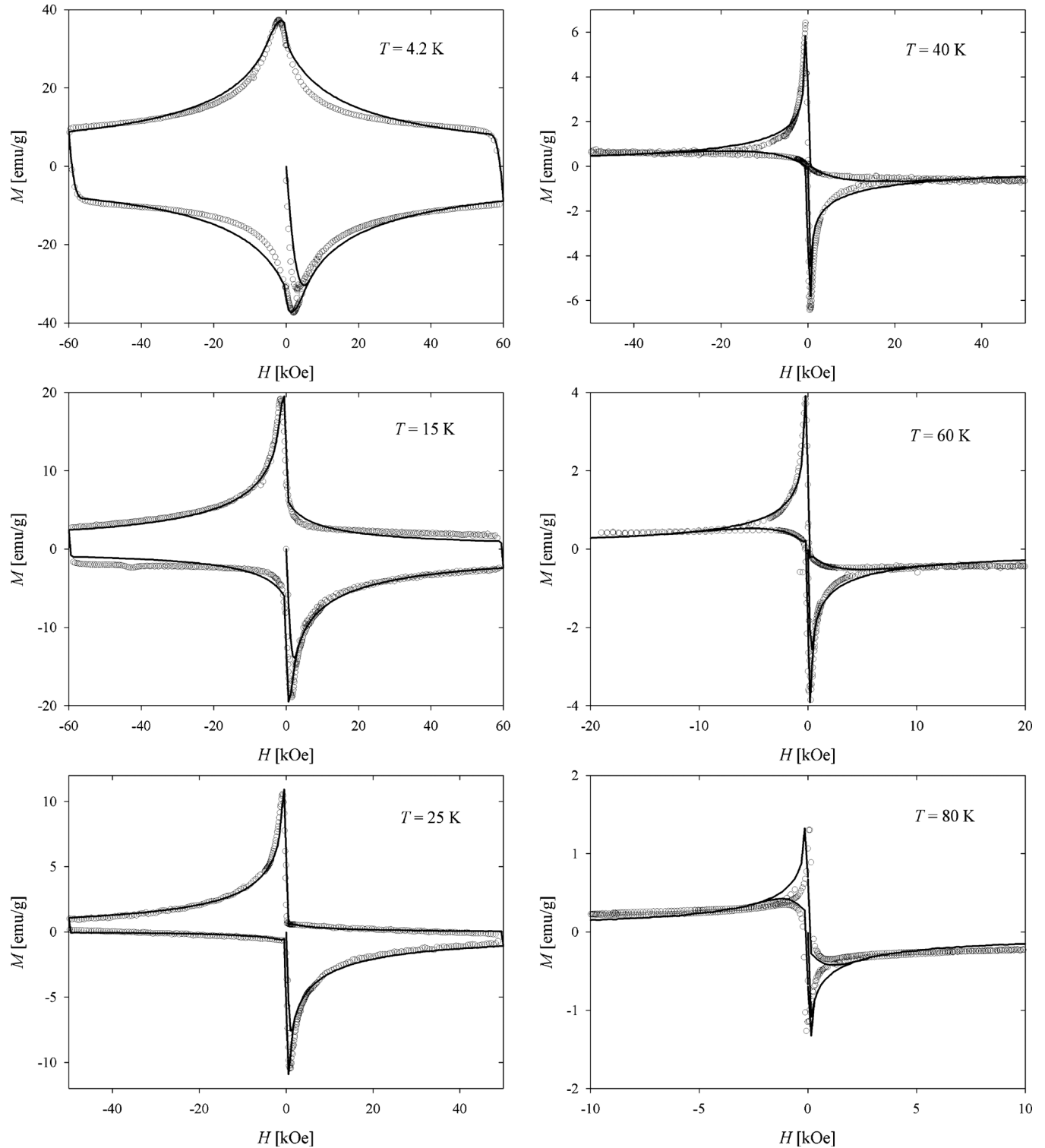
FIG. 2. Dependencies of magnetization M on magnetic field H of the porous Bi2223. Experimental data (symbols) and computed curves (solid lines).

changes from 0 to $l_s \geq R$. The value of l_s is believed to be about the London penetration depth λ.[6] Therefore, if a super-conducting crystal or grains in a polycrystalline sample have a size smaller than 2λ then pinning is expected to be missing in all volume and the $M(H)$ dependencies are reversible at any temperature.

III. EXPERIMENT

Synthesis of a porous $Bi_{1.8}Pb_{0.3}Sr_{1.9}Ca_2Cu_3O_x$ (Bi2223) is described in Ref. 14. This material is formed by disordered and unpacked flakeslike crystallites with the width of ~ 1 μm and the lengthwise sizes of ~ 20 μm. The density of the porous Bi2223 is equal to 1.6 g/cm^3. The temperature of superconducting transition is 113 K.

The textured Bi2223 was prepared from the porous one.[15] The textured ceramics with the texture degree of 0.97 consists of ordered crystallites with the sizes of ~ 1 μm along the c axis and ~ 10–20 μm in the ab plane. The density of textured Bi2223 is equal to 5.3 g/cm^3.
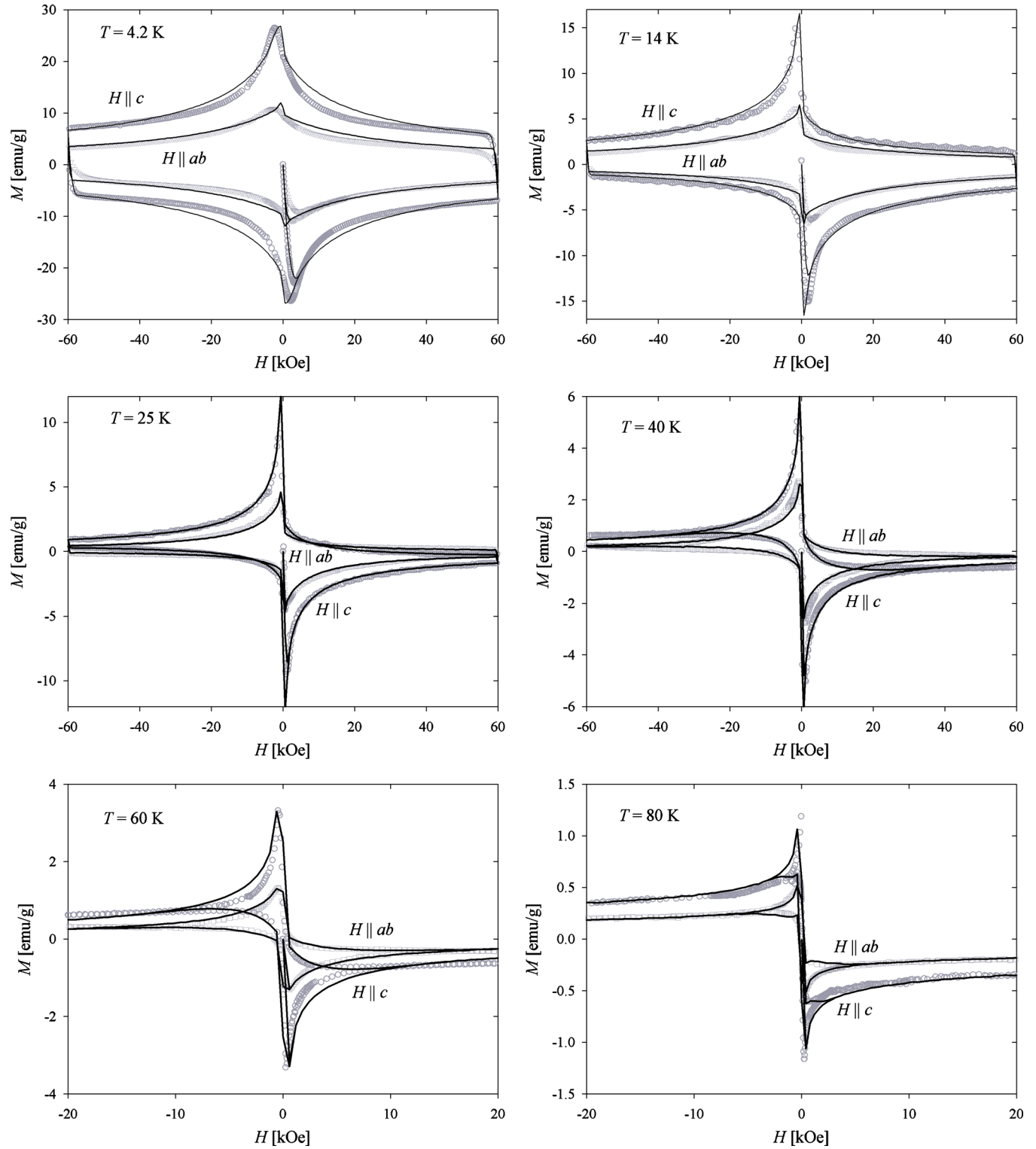
FIG. 3. (Color online) Dependencies of magnetization M on magnetic field H of the textured Bi2223. Experimental data (symbols) and computed curves (solid lines).

Samples for magnetic measurements had cubic form with the edges of 1.6 mm. The $M(H)$ dependencies were measured at temperatures of 4.2, 14, 25, 40, 60, and 80 K. The textured samples were investigated in two orientations of field H relative to the predominant direction of the crystallites in the textured sample: the magnetic field is directed perpendicularly to the texturing plane ($H\|c$) and along the texturing plane ($H\|ab$).

Figure 2 demonstrates the magnetization loops of the porous Bi2223 measured at temperatures (T) of 4.2–80 K. Figure 3 demonstrates the magnetization loops of the textured Bi2223 measured at temperatures of 4.2–80 K for $H\|c$ and $H\|ab$. For the $M(H)$ dependencies at $T=40$, 60, and 80 K, values of the irreversibility field $H_{irr}(T)$ are smaller than the maximal applied field $H_m=60$ kOe. At any fixed temperature, H_{irr} of the porous Bi2223 is smaller than the irre-
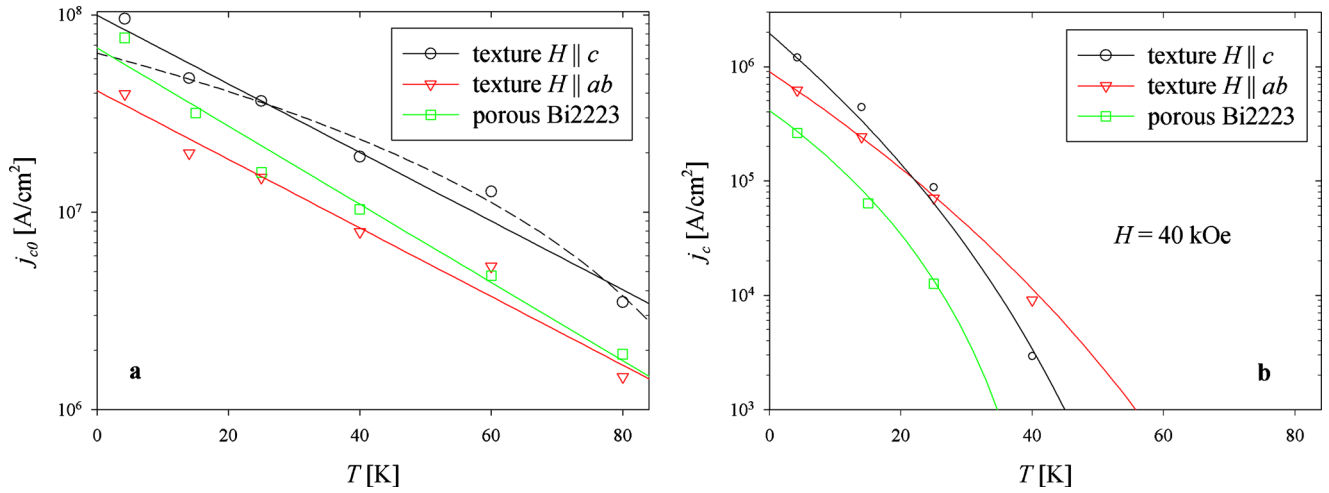
FIG. 4. (Color online) Semilog plots of temperature dependencies of critical current density j_c at $H=0$ (a) and $H=40$ kOe (b). Experimental data (symbols) and fitting curves $j_c(T)=j_c(0)\exp(-T/T^*)$ (solid lines) and $j_c(T)=j_c(0)(1-T/T^*)^n$ (dashed lines).

versibility fields of the textured Bi2223 and for the textured Bi2223 H_{irr} for $H\|c$ is smaller than H_{irr} for $H\|ab$. The $M(H)$ dependencies of the textured Bi2223 are scaled according to $M^{H\|c}(H)=\gamma M^{H\|ab}(\gamma H)$ (Ref. 16) with the anisotropy coefficient $\gamma=2.4$. Results of the detailed investigation of anisotropy of the texture will be presented in the other work.

The experimental $M(H)$ dependencies demonstrate that the asymmetry increases with temperature and field. At $T=4.2$ K the magnetization loops are nearly symmetric relative to the $M=0$ axis at fields of 10–55 kOe but at higher temperatures the magnetization loops are distinctly asymmetric. At $T=80$ K the $M(H)$ dependencies are reversible for the porous Bi2223 at fields higher than 1.5 kOe and for the textured Bi2223 at fields higher than 2 kOe for $H\|c$ and 4 kOe for $H\|ab$.

IV. DISCUSSION

The experimental data were fitted in the frame of the developed model. The main fitting parameters are the depth of surface equilibrium layer l_s and the product of j_c and the average granule radius R. We used the simple dependence $l_s(H)=l_s(0)[1+H/(0.3H_{irr})]$ that works good for all described curves at any T. The calculated magnetization loops depends very slightly on different distribution functions $\varphi(R)$ for both the textured Bi2223 and the porous Bi2223 such that we disregarded a dispersion of the granule parameters.

In Figs. 2 and 3 the computed curves are displayed together with the experimental loops. There is the good agreement between the presented data at all temperatures. Some discrepancy may be due to a demagnetizing factor of the sample and grains.[17] The textured Bi2223 magnetization dependencies were fitted with the $j_c(B)$ dependence (4), where $Q=5$, $g\approx 0.85-1$. The characteristic scale induction B_0 decreases from $\sim 2.5(H\|c)$, 5 kOe ($H\|ab$) at $T=4.2$ K to $\sim 0.2(H\|c)$, 0.4 kOe ($H\|ab$) at $T=80$ K. Next scale B_1 changes from 0.04 kOe ($H\|c$), 0.02 kOe ($H\|ab$) to 0.3 kOe ($H\|c$), 0.4 kOe ($H\|ab$). The porous Bi2223 magnetization dependencies were fitted with similar $j_c(B)$ parameters as for the textured sample, $H\|c$.

Figure 4 shows the temperature dependence of the criti-

cal current density estimated with $R=10$ μm for textured Bi2223 and $R=20$ μm for the porous Bi2223. The $j_{c0}(T)$ data in Fig. 4(a) estimated from the $M(H)$ fit. Similar fast, exponential-like, j_c decreasing was observed on Bi2223 samples.[18] The Kim–Anderson model for the flux creep and the collective pinning model[19] do not describe the $j_c(T)$ obtained. An empirical scaling relation $j_c(T)=j_c(0)(1-T/T_c)^n$, which with the parameter $n=3/2$ is the same as the Ginzburg–Landau theory in dirty limit near T_c,[20] is used commonly for the temperature dependence of critical current density of high-T_c superconductors. This formula describes the estimated $j_{c0}(T)$ data for temperature range higher than 20 K with $n=2.3$ for the textured sample (both $H\|c$ and $H\|ab$) and $n=3$ for the porous sample. The exponential dependency $j_c(T)=j_c(0)\exp(-T/T^*)$ fits the $j_{c0}(T)$ data satisfactory with the parameter $T^*=25$ K for the textured sample (both $H\|c$ and $H\|ab$) and $T^*=22$ K for the porous sample [Fig. 4(a)]. Figure 4(b) demonstrates the $j_c(T)$ dependencies at $H=40$ kOe obtained from the Bean formula j_c [A/cm²] $=30(M^+-M^-)$ [emu/cm³]/(2R[cm]). The $j_c(T)$ dependencies in Fig. 4(b) are fitted good by $j_c(T)=j_c(0)(1-T/T^*)^n$ with $n=9$ for the textured Bi2223 ($T^*=79$ K for $H\|c$ and $T^*=106$ K for $H\|ab$) and $n=4.5$, $T^*=47$ K for the porous Bi2223.

The value of the fitted l_s at $H=0$ grows from $l_s=200$ nm at $T=4.2$ K to $l_s\sim 3000$ nm at $T=80$ K [see Fig. 5(a)]. For all samples, at $H=40$ kOe the average radius R is smaller than values of l_s at low temperatures but l_s becomes greater than R at T above 40 K [Fig. 5(b)]. The $l_s(T)$ increase in Fig. 5(b) correlates with the $j_c(T)$ decrease in Fig. 4(b) that is due to M^+ approaches to M^- whereas l_s/R goes to 1.

V. CONCLUSION

In conclusion, the magnetization loops of porous and textured Bi2223 were measured in fields up to 60 kOe at different temperatures. The $M(H)$ dependence asymmetry increases with increasing temperature. To describe the asymmetric magnetization loops, the extended variant of the critical state model was developed. In the presented model, the
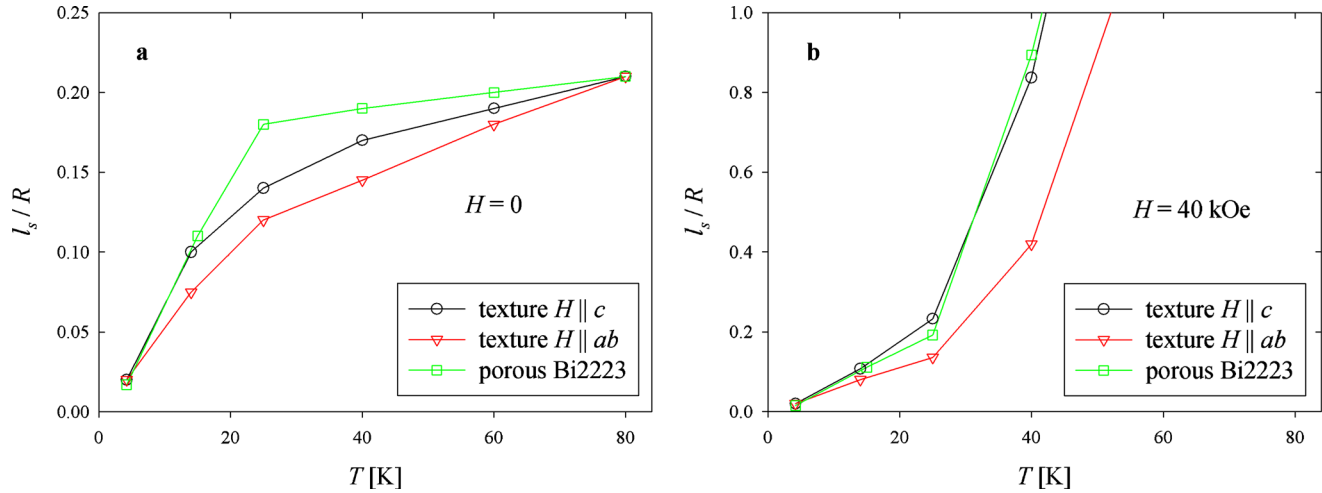
FIG. 5. (Color online) Temperature dependence of boundary depth l_s, divided by the average radius of granule R, at $H=0$ (a) and $H=40$ kOe (b).

asymmetry is referred to the single parameter l_s, which determines the position of the boundary between the surface layer with the thermal equilibrium magnetization, and the central region with the critical state magnetization. The equilibrium surface layer is formed due to the inhomogeneous distribution of magnetic field and pinning force in the sample. As following from the model proposed, the $M(H)$ dependence of the sample consisting of sufficiently small superconducting granules ($\sim\lambda$) should be fully reversible at all temperatures.

ACKNOWLEDGMENTS

[1]A. Sanchez and C. Navau, Phys. Rev. B **64**, 214506 (2001).
[2]A. Palau, T. Puig, X. Obradors, and Ch. Jooss, Phys. Rev. B **75**, 054517 (2007).
[3]M. L. Hodgdon, J. Appl. Phys. **69**, 4904 (1991).
[4]B. Schulz, B. Schliepe, W. Wisny, and K. Baberschke, Physica C **199**, 356 (1992).
[5]L. Ji, M. S. Rzchowski, N. Anand, and M. Tinkham, Phys. Rev. B **47**, 470 (1993).
[6]D. X. Chen, R. W. Cross, and A. Sanchez, Cryogenics **33**, 695 (1993); D. X. Chen, R. B. Goldfarb, R. W. Cross, and A. Sanchez, Phys. Rev. B **48**, 6426 (1993).
[7]W. A. Fietz, M. R. Beasley, J. Silcox, and W. W. Webb, Phys. Rev. **136**, A335 (1964).
[8]M. Sinder, V. Meerovich, V. Sokolovsky, and I. Vajda, IEEE Trans. Appl. Supercond. **9**, 4661 (1999).
[9]V. M. Krasnov and V. V. Ryazanov, Physica C **297**, 153 (1998).
[10]Y. Kimishima and Y. Ichiyanagi, Physica C **353**, 111 (2001).
[11]Y. Kimishima, H. Ichikawa, S. Takano, and T. Kuramoto, Supercond. Sci. Technol. **17**, S36 (2004).
[12]V. V. Val'kov and B. P. Khrustalev, Sov. Phys. JETP **80**, 680 (1995).
[13]D. M. Gokhfeld, D. A. Balaev, S. I. Popkov, K. A. Shaykhutdinov, and M. I. Petrov, Physica C **434**, 135 (2006).
[14]M. I. Petrov, T. N. Tetyueva, L. I. Kveglis, A. A. Efremov, G. M. Zeer, K. A. Shaykhutdinov, D. A. Balaev, S. I. Popkov, and S. G. Ovchinnikov, Tech. Phys. Lett. **29**, 986 (2003); D. A. Balaev, I. L. Belozerova, D. M. Gokhfeld, L. V. Kashkina, Yu. I. Kuz'min, C. R. Michel, M. I. Petrov, S. I. Popkov, and K. A. Shaykhutdinov, Phys. Solid State **48**, 207 (2006).
[15]M. I. Petrov, D. A. Balaev, I. L. Belozerova, A. D. Vasil'ev, D. M. Gokhfeld, O. N. Martyanov, S. I. Popkov, and K. A. Shaykhutdinov, Tech. Phys. Lett. **33**, 740 (2007).
[16]Z. Hao, J. R. Clem, J. H. Cho, and D. C. Johnston, Physica C **185–189**, 1871 (1991); Z. Hao and J. R. Clem, Phys. Rev. B **46**, 5853 (1992).
[17]Kh. R. Rostami, Sov. Phys. JETP **107**, 612 (2008).
[18]B. Hensel, G. Grasso, and R. Flükiger, Phys. Rev. B **51**, 15456 (1995).
[19]T. Higuchi and S. I. Yoo, Phys. Rev. B **59**, 1514 (1999).
[20]J. R. Clem, B. Bumble, S. I. Raider, W. J. Gallagher, and Y. C. Shih, Phys. Rev. B **35**, 6637 (1987).